

DETERMINATION OF FLOW PATTERN AND ITS EFFECT ON NO_x EMISSION IN A TANGENTIALLY FIRED SINGLE CHAMBER SQUARE FURNACE

by

Shahram KHALILARYA and Amin LOTFIANI *

Department of Mechanical Engineering, Urmia University, Urmia, Iran

Original scientific paper
UDC: 662.613.5:533.6.011:517.957
DOI: 10.2298/TSCI1002493K

Tangentially fired furnaces are vortex combustion units which have become more attractive in the field of power station firing systems in recent years. Although the application of tangentially fired furnace continuously increases, they have not yet been adequately investigated. The present work provides a numerical study of flow pattern and its effect on NO_x emission in a single chamber square tangentially fired furnace. Details of the flow field, along with temperature and species concentration contour maps are obtained from the solution of the conservation equations of mass, momentum, and energy, and transport equations for scalar variables in addition to the equations of the turbulence model. Four cases with different inlet air velocities are studied. Combustion in a natural gas-fired horizontal furnace with circular cross-section is simulated to verify the simulation methodology and the solution algorithm. Results are compared with those of the existing references and good agreement is observed. Calculations for the tangentially fired furnace show that while the vortex created in the center of the furnace becomes stronger as the burner outlet air velocity increases, its size remains almost unchanged. Highest-temperature regions are favorably far from the furnace walls so that erosion and local over-heating can be minimized. According to the results, higher inlet air velocities lead to more uniform temperature distributions with lower peak temperatures, which in turn result in remarkable reduction of NO_x emission of the furnace.

Key words: *tangential firing, diffusion flame, furnace, NO_x emission, CFD*

Introduction

Tangentially fired furnaces (TFF) are units of polygon shape with four, six, eight, or more sides. In these furnaces fuel and air are admitted in a tangential manner from the furnace sides and the flames are directed at an imaginary circle in the middle of the furnace [1-4]. This brings about a vortex motion which would be by itself moving upwards. Therefore TFF are essentially vortex combustion units. The size of this vortex depends mainly on dimensions of the furnace. Stable burning in TFF is achieved by the arrangement of the burners rather than by the individual burners. When a furnace is fired tangentially, each flame impinges upon the adjacent

* Corresponding author; e-mail: a.lotfiani@urmia.ac.ir, amn622002@yahoo.com

flame, creating a recirculating flow and stabilizing the latter flame. Hence the precise control over local air/fuel ratio is not necessary because lean or rich zones become entrained in the vortex and are blended for efficient combustion.

In recent years, TFF have become more attractive in the field of power station firing systems and other similar applications. They have been used extensively throughout the world with wide applications in low and high capacity steam boilers [4-6]. These furnaces are quite suitable for many types of fuels including coal, oil, and gas. Characteristic features of TFF refer especially to desirable mixing and heat distribution inside the furnace, and low NO_x emission. Efficient mixing ensures reliable combustion with uniform temperature distribution and relatively high temperature in the core. Consequently there is uniform heat flux to the furnace walls. Tangentially fired units are currently being designed with single or double chamber furnaces which can be characterized by square, rectangle, or polygon horizontal cross-sections. Although the application of TFF continuously increases, they have not yet been adequately investigated. A number of trials have been made; some of them are introduced in the following.

Tong *et al.* [1, 2] studied the effect of the imaginary circle diameter and the initial flow field on the aerodynamic field in a TFF by numerical simulation and experiments in the cold model. Moreover, a new kind of grid arrangement was proposed in their work in order to reduce the false diffusion at the exit zone of burner. They also studied the effect of the side secondary air velocity on the aerodynamic field in a TFF both numerically and experimentally. Zhou *et al.* [3, 4] presented a computational study on the optimization of the operating conditions of a full-scale TFF. In a separate work, they proposed a two-stage simulation method for obtaining temperature distribution in the furnace of a tangentially fired boiler. El-Mahallawy and his research group [5, 6] investigated the effect of destabilization of the flame of one burner on the other flames in the furnace. Flow field and thermal characteristics of a model TFF under different conditions of burner tripping were determined. They also studied the effect of the burners' deviation angle from the furnace diagonals on the furnace performance. Their work represents the most detailed reference to assist the development and validation of mathematical models of TFF. Li *et al.* [7] compared NO_x emission reductions with different air staging techniques in tangentially fired boilers. Zhou *et al.* [8] presented experimental and numerical study on the aerodynamic field in the upper furnace of a tangentially fired boiler.

The objective of this work is to obtain flow pattern and study its effect on NO_x emission of a square TFF. For this purpose, four cases with different inlet air velocities are studied. Combustion in a natural gas-fired horizontal furnace with circular cross-section is simulated to verify the simulation methodology and the solution algorithm. Results are compared with those of the existing references and good agreement is observed.

Problem specifications

In the present paper, a single chamber square TFF has been studied. Furnace geometry and dimensions along with the co-ordinate system used are shown in fig. 1. Side length of the horizontal cross-section square of the furnace is 850 mm and the height is 1000 mm. The furnace is surrounded at all sides by a water-cooling jacket, so that the furnace walls are at constant temperature of 350 K. Each of the four sides of the furnace accommodates a methane burner.

The burners have been arranged in such a way that the imaginary circle diameter is 75 mm. All the burners are mounted at a distance of 370 mm from the bottom of the furnace. Flue gases exit through a 50 mm high cylindrical vent of 200 mm diameter at the top of the fur-

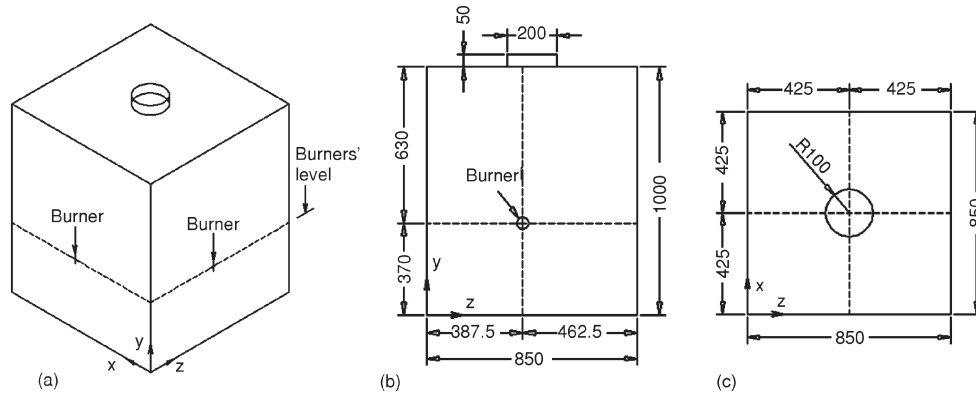


Figure 1. Furnace geometry and dimensions and the co-ordinate system used (dimensions in mm);
 (a) 3-D view, (b) side view, (c) top view

nace. Each burner exit consists of two coaxial pipes. The diameter of the inner pipe is 5 mm. Fuel flows through the inner pipe while air is admitted through the annular gap created by the coaxial pipes. Details of a burner outlet are given in fig. 2.

In this work, four different cases have been investigated in order to understand the influence of air velocity at the burner exit on flow pattern and, in turn, on NO_x emission of the furnace. In all cases, fuel type (*i. e.* methane), the overall equivalence ratio (*i. e.* the ratio of fuel-to-air to stoichiometric fuel-to-air), flow rates of fuel and air, fuel and air temperatures, and fuel velocity at the burner exit stay the same. Burner outlet air velocity (and thus outer pipe diameter) is the only parameter that is changed. Required data are listed in tab. 1.

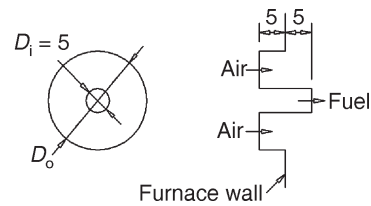


Figure 2. Schematic views of a burner exit (dimensions in mm)

Table 1. Values of different parameters in each case

	Case 1	Case 2	Case 3	Case 4
Overall equivalence ratio	0.75	0.75	0.75	0.75
Air flow rate [m ³ s ⁻¹]	0.079482	0.079482	0.079482	0.079482
Fuel flow rate [m ³ s ⁻¹]	6.283·10 ⁻³	6.283·10 ⁻³	6.283·10 ⁻³	6.283·10 ⁻³
Inlet air velocity [ms ⁻¹]	10	20	40	80
Inlet fuel velocity [ms ⁻¹]	80	80	80	80
Outer pipe diameter [mm]	50.547	35.9166	25.642	18.473
Inner pipe diameter [mm]	5	5	5	5
Inlet air temperature [K]	300	300	300	300
Inlet fuel temperature [K]	300	300	300	300

Mathematical model

The mathematical model is based on the solution of the governing equations of flow (*i. e.* mass and momentum equations), turbulence, chemical species and energy. Then NO_x formation is predicted in a separate step from the solution of NO species transport equation. This is justified on the grounds that the NO concentrations are very low and have negligible impact on the hydrocarbon combustion prediction [9, 10]. The turbulence model used to determine the turbulent viscosity is the two-equation realizable k - ε model proposed by Shih *et al.* [9]. This model is the most suitable one among the two-equation eddy viscosity turbulence models for simulating gaseous round jets and combustion problems of the present type [11, 12]. Turbulence-chemistry interaction is taken into account using the eddy-dissipation model. In this model, reaction rates are assumed to be controlled by turbulent mixing, so expensive Arrhenius chemical kinetic calculations are avoided. The combustion is modeled using a global one-step reaction mechanism, assuming complete conversion of the fuel to CO₂ and H₂O. The formation of thermal NO_x is determined by the Zeldovich mechanism. The prompt NO_x contribution to total NO_x from stationary combustors is small. However, as NO_x emissions are reduced to very low levels by employing new strategies, the relative importance of the prompt NO_x is expected to increase [7, 13, 14]. In this study, the prompt NO_x is also taken into account. Since all the above-mentioned governing equations are presented in many references (*e. g.* see [3, 6, 8, 15]), they are not reviewed here except for NO_x formation submodel.

As cited, formation of thermal NO_x is determined by the Zeldovich mechanism which is a set of highly temperature-dependent chemical reactions. The sequence is complicated, but the following two steps represent the essential features [9]:



These sequences sum to the overall reaction of one nitrogen and one oxygen molecule producing two nitric oxide molecules as follows:



The net rate of formation of NO via reactions (1) and (2) is given by:

$$\frac{d[\text{NO}]}{dt} = 2k_{f,1}[\text{O}][\text{N}_2] - \frac{k_{r,1}k_{r,2}[\text{NO}]^2}{k_{f,1}[\text{N}_2]k_{f,2}[\text{O}_2]} - \frac{k_{r,1}[\text{NO}]}{k_{f,2}[\text{O}_2]} \quad (4)$$

where $k_{f,1}$ and $k_{f,2}$ are the rate constants for the forward reactions 1 and 2, respectively, and $k_{r,1}$ and $k_{r,2}$ are the corresponding reverse rate constants. This equation is based on the quasi-steady assumption according to which the rate of consumption of free nitrogen atoms becomes equal to the rate of its formation when there is sufficient oxygen (fuel-lean flame).

To solve eq. (4), concentration of O atoms is required in addition to concentration of stable species (*i. e.* O₂ and N₂). In this work, the partial equilibrium approach is used to determine the O radical concentration. This approach is an improvement to the method suggested by Zeldovich, namely equilibrium approach. Concentration of O atoms is obtained from:

$$[O] = 36.64 \sqrt{[O_2] T} e^{-\frac{27123}{T}} \quad (5)$$

where T is in Kelvin and $[O]$ is in $[gmol\ m^{-3}]$. The above expression generally leads to a higher O radical concentration than the equilibrium value. In terms of the transport equation for NO, the NO source term due to thermal NO_x mechanism is:

$$S_{\text{thermal,NO}} = M_{\text{NO}} \frac{d[\text{NO}]}{dt} \quad (6)$$

Here M_{NO} is the molecular weight of NO and $d[\text{NO}]/dt$ is computed from eq. (4).

Formation of prompt NO_x involves a complex series of reactions and many possible intermediate species. The route now accepted is as follows [9]:



A number of species resulting from fuel fragmentation have been suggested as the source of prompt NO_x in hydrocarbon flames (*e. g.* CH, CH₂, C, and C₂H), but the major contribution is from CH, and CH₂ via:



The products of these reactions could lead to formation of amines and cyano compounds that subsequently react to form NO.

Numerical solution

The numerical simulations are carried out using the commercial flow solver FLUENT 6.2.16 based on the finite volume method. All the governing equations are discretized using the first-order upwind scheme. The discretized equations are solved using the SIMPLE algorithm. The implicit and segregated solver is applied for the solution of the system of governing equations. The commercial package GAMBIT 2.2.30 was employed to generate the geometry and mesh for the computational domain. Tetrahedral/hybrid elements are used for meshing the geometry. The unstructured meshes generated for the simulation of the four cases of interest (see tab. 1) consist of 53638 elements for case 1, 53707 elements for case 2, 54009 elements for case 3, and 52646 elements for case 4. In order to obtain accurate results the size of the elements is reduced near the nozzles where large gradients are expected [16-18]. An example of the generated meshes is shown in fig. 3.

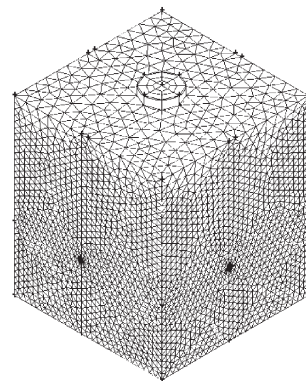


Figure 3. An example of the computational grids consisting of tetrahedral/hybrid elements

Different types of boundary conditions are used for different zones of the flow domain. Velocity inlet boundary condition is used at the fuel and air inlets and pressure outlet boundary condition is used at the furnace outlet. Wall boundary condition with constant temperature of 350 K and no-slip condition is used at the walls.

Results and discussion

In order to verify the simulation methodology and the solution algorithm, combustion in a natural gas-fired horizontal furnace with circular cross-section is simulated. Combustion chamber of this furnace is a cylindrical enclosure of 293 mm radius and 990 mm length. The fuel is injected from a central nozzle whereas the primary air enters from an annulus. The secondary air is inserted axially in the direction of the primary air supply from a second annulus. Inlet fuel and air both enter the combustion chamber at 295 K. Furnace geometry and dimensions along with the co-ordinate system used are illustrated in fig. 4. Inlet fuel and air velocities and other required data are listed in tab. 2. A two-

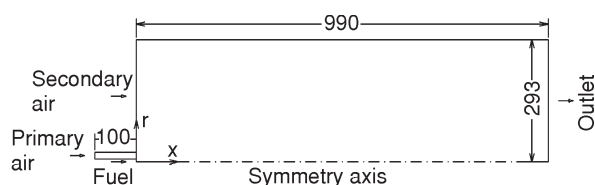


Figure 4. Geometry and dimensions of the axisymmetric furnace investigated for validation of the present work along with the co-ordinate system used

Table 2. Axisymmetric furnace inlet fuel and air velocities and other required data

Fuel inlet [mm]	$r = 0-3.0$
Primary air inlet [mm]	$r = 7.5-22.5$
Secondary air inlet [mm]	$r = 22.5-293.0$
Fuel velocity at inlet [ms^{-1}]	21.9
Primary air velocity at inlet [ms^{-1}]	5.0
Secondary air velocity at inlet [ms^{-1}]	0.3

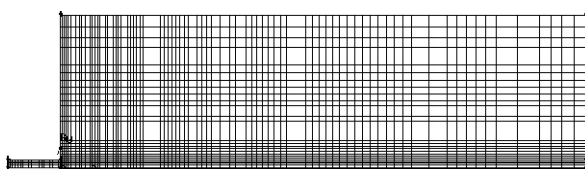


Figure 5. Computational grid generated for the investigation of the axisymmetric furnace

dimensional mesh consisting of 3763 quadrilateral cells is generated to study the above-mentioned furnace. A dense grid is carefully assigned around the furnace centerline and near the inlets where large gradients are expected, to increase the solution accuracy [16-18]. This is shown in fig. 5. Results are compared with those of reference [16] and reasonable agreement is observed. As a sample of the results, temperature distribution along the furnace centerline is presented in fig. 6. No significant difference is observed between the temperature profiles predicted by the two works. Maximum temperature on the furnace centerline predicted by the present work is a little more than that predicted by reference [16]. This is possibly attributed to the performance of the combustion model.

Velocity vectors at the burners' level ($y = 370$ mm) are shown in fig. 7. This figure compares the flow pattern in the four different cases. It can be seen that the clockwise vortex motion in the center of the furnace becomes stronger as the burner outlet air velocity increases. The size of this vortex is not affected by the burner exit air velocity. Due to momentum diffusion, the

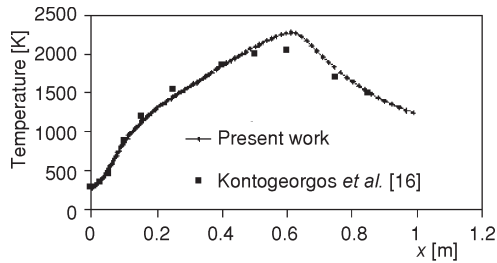


Figure 6. Comparison of predicted temperature distributions along the furnace centerline for validation of the present work

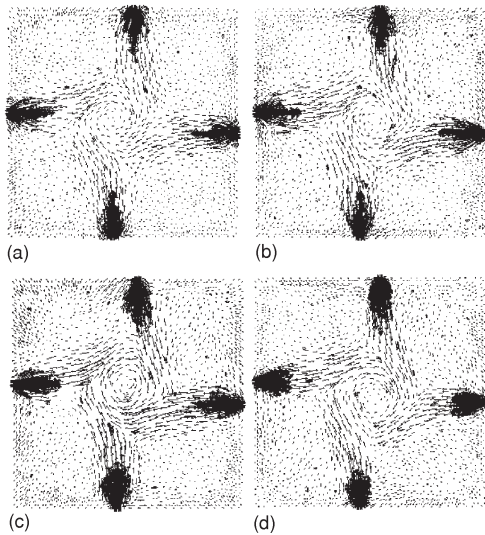


Figure 7. Flow pattern at the burners' level in the four different cases
 (a) case 1, (b) case 2, (c) case 3, (d) case 4

velocity magnitudes are greatly reduced as the flames reach the center of the furnace. Arrangement of the burners serves to stabilize burning in the furnace. Each flame impinges upon the adjacent flame creating a recirculating flow and stabilizing the latter flame. Figure 8 shows the flow pattern at $z = 387.5$ mm in the four different cases. As shown in this figure, there are

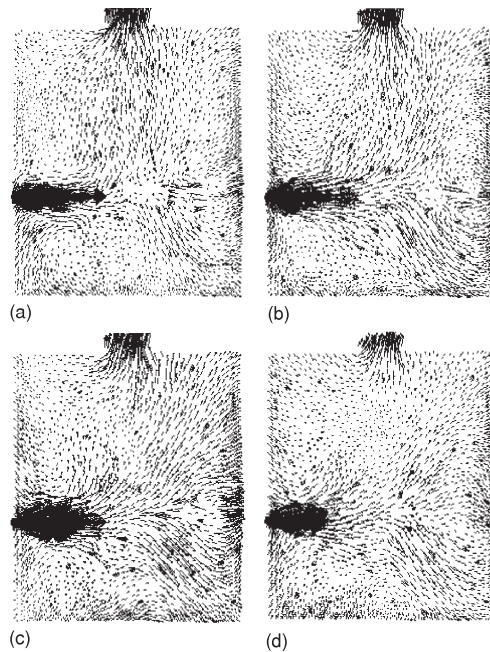


Figure 8. Flow pattern at $z = 387.5$ mm in the four different cases
 (a) case 1, (b) case 2, (c) case 3, (d) case 4

recirculation regions near the burners' outlets. These regions are more dominant below the nozzles. It must be noted that velocity vectors are small near the furnace walls. This can be seen in both figs. 7 and 8.

Contours of temperature in the four different cases are presented in figs. 9 and 10. Contour values in these figures are non-dimensionalized by the maximum temperature in case 4 (*i. e.* 1688 K). It can be found out that the maximum temperature decreases as the burner outlet air velocity rises. Peak dimensionless temperature is 1.20 in case 1, 1.06 in case 2, 1.05 in case 3, and 1.00 in case 4. It should be reminded that the overall equivalence ratio is kept constant (see tab. 1). As shown in figs. 9 and 10, temperature distribution is more uniform in cases with higher burner exit air velocity. Highest-temperature regions can be observed in the center of the furnace. Since these regions are sufficiently far from the furnace walls, erosion and local over-heating can be minimized.

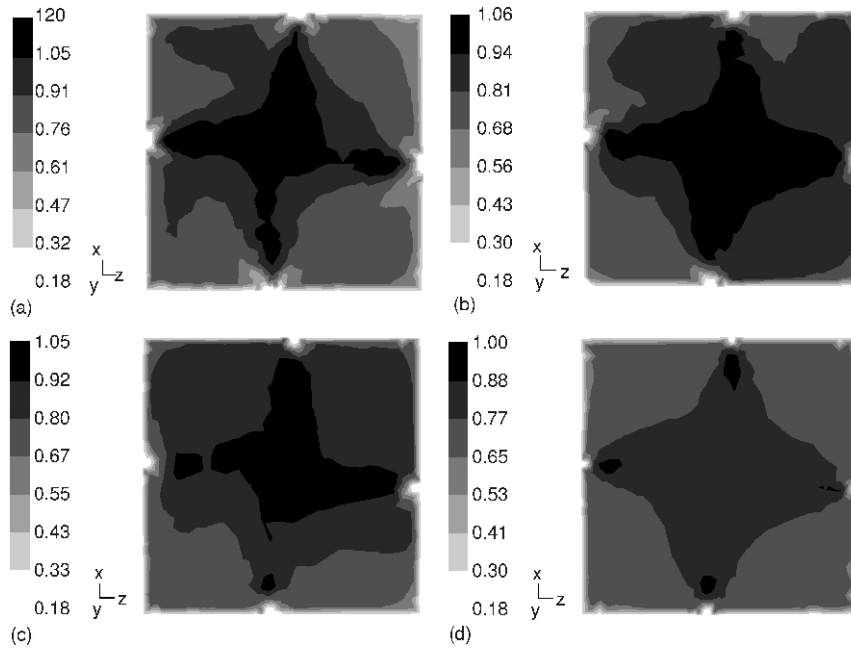


Figure 9. Contours of dimensionless temperature at the burners' level in the four different cases
(a) case 1, (b) case 2, (c) case 3, (d) case 4

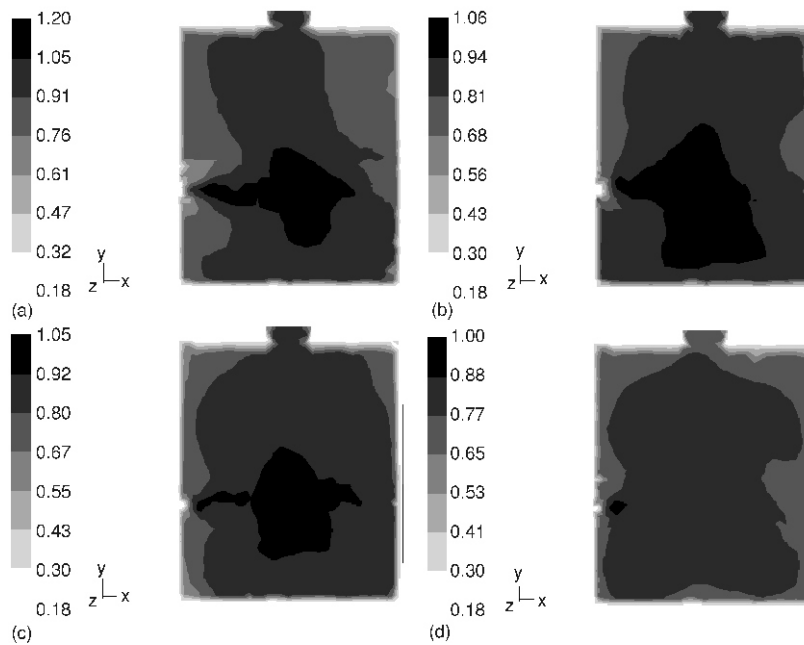


Figure 10. Contours of dimensionless temperature at $z = 387.5$ mm in the four different cases
(a) case 1, (b) case 2, (c) case 3, (d) case 4

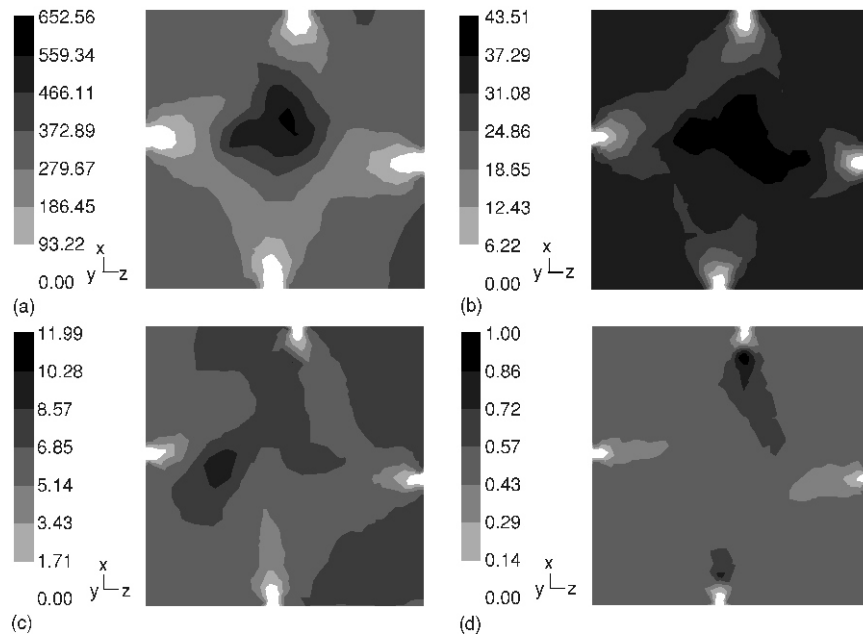


Figure 11. Contours of dimensionless NO concentration at the burners' level in the four different cases
(a) case 1, (b) case 2, (c) case 3, (d) case 4

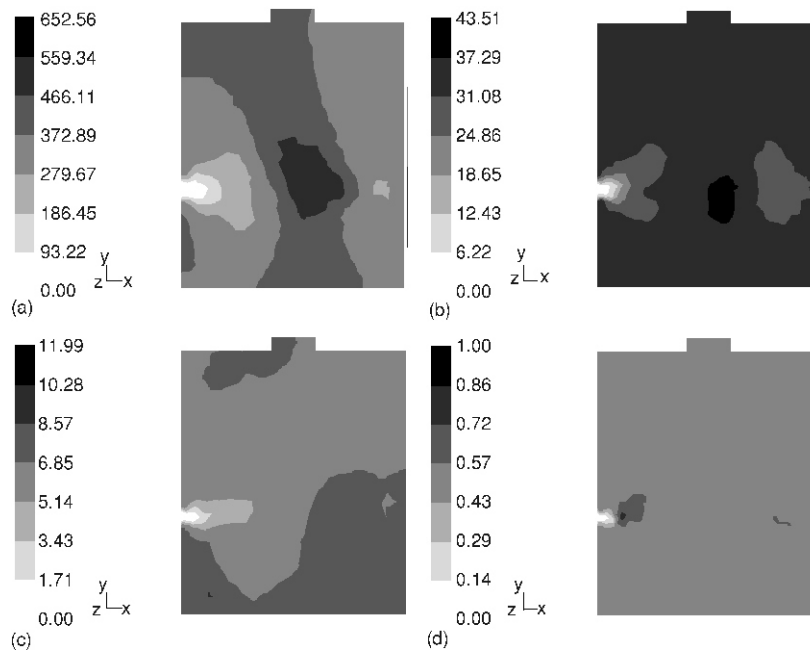


Figure 12. Contours of dimensionless NO concentration at $z = 387.5$ mm in the four different cases
(a) case 1, (b) case 2, (c) case 3, (d) case 4

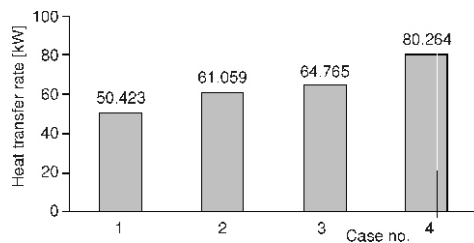


Figure 13. Rate of heat transfer to furnace walls in the four different cases

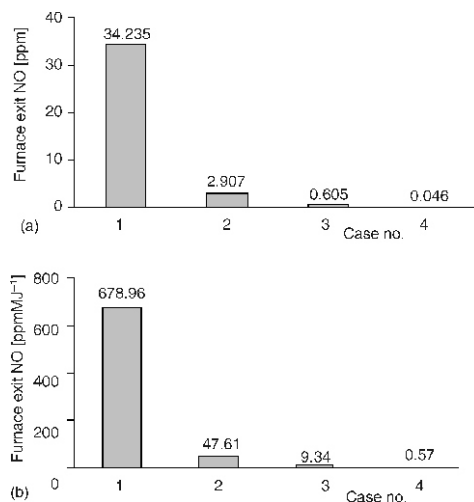


Figure 14. Mass-averaged NO at the furnace outlet in the four different cases

(a) in [ppm], (b) in [ppm·MJ⁻¹]

Contours of total NO concentration non-dimensionalized by the maximum NO concentration in case 4 (*i. e.* 0.089 ppm) are shown in figs. 11 and 12. Note that the contour values include both thermal and prompt NO. As can be observed, maximum dimensionless concentration of NO is 652.56 in case 1, 43.51 in case 2, 11.99 in case 3, and 1.00 in case 4. Increasing the burner outlet air velocity reduces the peak temperature and brings about a more uniform temperature distribution which consequently results in lower NO emission, as discussed earlier. As indicated in figs. 11 and 12, high concentrations of NO are observed in the center of the furnace, especially in regions with temperatures greater than about 1600 K. The rate of heat transfer to the furnace walls in the four different cases of interest is shown in fig. 13. Heat transfer rate rises from 50.423 kW in case 1 to 80.264 kW in case 4 as the inlet air velocity increases. Figure 14 demonstrates the furnace exit NO concentration in each case studied in this work. Figure 14(b) shows the furnace exit NO concentration in ppm per megajoule. In regard to this figure it can be found out that the mass-averaged NO concentration at the furnace outlet decreases significantly when the combustion air is admitted with higher velocities. The furnace exit NO concentration falls from 34.235 ppm in case 1 to 0.046 ppm in case 4.

Conclusions

Flow pattern and its effect on NO_x emission in a tangentially fired single chamber square furnace are determined. Four cases with different inlet air velocities are investigated. The overall equivalence ratio, fuel type (*i. e.* methane), flow rates of fuel and air, fuel and air temperatures, and fuel velocity at the burners' outlets remain unchanged in the four cases. Combustion in a natural gas-fired horizontal furnace with circular cross-section is simulated to verify the simulation methodology and the solution algorithm. Results are compared with those of the existing references and good agreement is observed. Calculations for the TFF show that while the vortex created in the center of the furnace becomes stronger as the burner outlet air velocity increases, its size is not affected. Velocity magnitudes are greatly reduced as the flames reach the center of the furnace due to momentum diffusion. Impingement of each flame upon the neighboring flame serves to create a vortex motion and thus stabilizes the combustion. Since highest-temperature regions in such combustion units are sufficiently far from the walls, erosion and

local over-heating can be minimized. Calculations show that higher inlet air velocities lead to more uniform temperature distributions with lower peak temperatures, which in turn result in remarkable reduction of NO emission.

References

- [1] Tong, Zh., *et al.*, Numerical Study of the Effect of Imaginary Circle Diameter and Initial Flow Field on the Aerodynamic Field in a Tangentially Fired Furnace, *J. of Thermal Science*, 6 (1997), 2, pp. 149-154
- [2] Tong, Zh., *et al.*, Study on the Effect of the Side Secondary Air Velocity on the Aerodynamic Field in a Tangentially Fired Furnace with HBC-SSA Burner, *J. of Thermal Science*, 8 (1999), 4, pp. 277-283
- [3] Zhou, N., Xu, Q., Zhou, P., Two-Stage Numerical Simulation for Temperature Profile in Furnace of Tangentially Fired Pulverized Coal Boiler, *J. Cent. South Univ. Technol.*, 12 (2005), 1, pp. 97-101
- [4] Zhou, P., Mei, Ch., Gong, G., Computational Study on Furnace Process in a Multi-Burner Boiler of Pulverized Coal Fired Tangentially at Four Corners, *J. Cent. South Univ. Technol.*, 7 (2000), 3, pp. 152-155
- [5] El-Mahallawy, F., El-Din Habik, S., *Fundamentals and Technology of Combustion*, Elsevier, Amsterdam, Boston, 2002
- [6] Habib, M. A., Ben-Mansour, R., Antar, M. A., Flow Field and Thermal Characteristics in a Model of a Tangentially Fired Furnace under Different Conditions of Burner Tripping, *Heat Mass Transfer*, 41 (2005), 10, pp. 909-920
- [7] Li, S., *et al.*, Comparison of NO_x Emission Reductions with Exclusive SOFA and CCOFA on Tangentially-fired Boilers, *Proceedings*, International Conference on Power Engineering, Hangzhou, China, 2007, pp. 805-809
- [8] Zhou, Y., *et al.*, Experimental and Numerical Study on the Flow Fields in Upper Furnace for Large Scale Tangentially Fired Boilers, *Applied Thermal Engineering*, 29 (2009), 4, pp. 732-739
- [9] ***, *Fluent 6.2 User's Guide*, Fluent Inc., Lebanon, NH 03766, USA, 2005
- [10] Blasiak, W., Fakhrai, R., Residence Time and Mixing Control in the Upper Furnace of Boilers and Incinerators, *Proceedings*, IT3'02 Conference, New Orleans, La., USA, 2002, pp. 1-10
- [11] Bakker, A., *Turbulence Models*, <http://www.bakker.org>
- [12] Khalilarya, S., Pourmahmod, N., Lotfiani, A., Evaluation of Two-Equation Turbulence Models for Simulation of Gaseous Round Jets (in Farsi), *Proceedings*, MEC 2009, Mashad, Iran, 2009, pp. 210-211
- [13] Han, X., *et al.*, Detailed Modeling of Hybrid Reburn/SNCR Processes for NO_x Reduction in Coal-Fired Furnaces, *Combustion and Flame*, 132 (2003), 3, pp. 374-386
- [14] Maloney, K., *et al.*, Computational Fluid Dynamic Modeling and Field Results for Co-Firing Gas over Coal in a Stoker Boiler, *Proceedings*, International Conference on Power Engineering, Hangzhou, China, 2007, pp. 886-892
- [15] Pathak, M., Dewan, A., Dass, A. K., Computational Prediction of a Slightly Heated Turbulent Rectangular Jet Discharged into a Narrow Channel Crossflow Using Two Different Turbulence Models, *International Journal of Heat and Mass Transfer*, 49 (2006), 21-22, pp. 3914-3928
- [16] Kontogeorgos, D. A., Keramida, E. P., Founti, M. A., Assessment of Simplified Thermal Radiation Models for Engineering Calculations in Natural Gas-fired Furnace, *International Journal of Heat and Mass Transfer*, 50 (2007), 25-26, pp. 5260-5268
- [17] Cumber, P. S., Fairweather, M., Evaluation of Flame Emission Models Combined with the Discrete Transfer Method for Combustion System Simulation, *International Journal of Heat and Mass Transfer*, 48 (2005), 25-26, pp. 5221-5239
- [18] Kumar, S., Paul, P. J., Mukunda, H. S., Prediction of Flame Liftoff Height of Diffusion/Partially Premixed Jet Flames and Modeling of Mild Combustion Burners, *Combust. Sci. and Tech.*, 179 (2007), 10, pp. 2219-2253

Paper submitted: October 5, 2009

Paper revised: November 2, 2009

Paper accepted: December 18, 2009